Journal of Statistical Physics, Vol. 30, No. 3, 1983

Analytic Study of Power Spectra of the Tent Maps near Band-Splitting Transitions

H. Shigematsu,[1] H. Mori,[1] T. Yoshida,[1] and H. Okamoto[1]

Received August 6, 1982

Successive band-splitting transitions occur in the one-dimensional map $x_{i+1} = g(x_i)$, $i = 0, 1, 2, \cdots$ with $g(x) = \alpha x$, $(0 \leqslant x \leqslant 1/2) - \alpha x + \alpha$, $(1/2 < x \leqslant 1)$ as the parameter α is changed from 2 to 1. The transition point from N $(= 2^n)$ bands to $2N$ bands is given by $\alpha = (\sqrt{2})^{1/N}$ $(n = 0, 1, 2, \cdots)$. The time-correlation function $\xi_i \equiv \langle \delta x_i \, \delta x_0 \rangle / \langle (\delta x_0)^2 \rangle$, $\delta x_i \equiv x_i - \langle x_i \rangle$ is studied in terms of the eigenvalues and eigenfunctions of the Frobenius–Perron operator of the map. It is shown that, near the transition point $\alpha = \sqrt{2}$, $\xi_i \simeq [(10 - 4\sqrt{2})/17] \delta_{i,0} - [(10\sqrt{2} - 8)/51]\delta_{i,1} + [(7 + 4\sqrt{2})/17](-1)^i e^{-\gamma i}$, where $\gamma \equiv \sqrt{2}(\alpha - \sqrt{2})$ is the damping constant and vanishes at $\alpha = \sqrt{2}$, representing the critical slowing-down. This critical phenomenon is in strong contrast to the topologically invariant quantities, such as the Lyapunov exponent, which do not exhibit any anomaly at $\alpha = \sqrt{2}$. The asymptotic expression for ξ_i has been obtained by deriving an analytic form of ξ_i for a sequence of α which accumulates to $\sqrt{2}$ from the above. Near the transition point $\alpha = (\sqrt{2})^{1/N}$, the damping constant of ξ_i for $i \geqslant N$ is given by $\gamma_N = \sqrt{2}(\alpha^N - \sqrt{2})/N$. Numerical calculation is also carried out for arbitrary α and is shown to be consistent with the analytic results.

KEY WORDS: Chaos; mapping; ergodic; mixing; time-correlation function; chaos–chaos transition; Frobenius–Perron operator.

1. INTRODUCTION

It has turned out for many physical systems that an essential feature of chaos can be represented by a one-dimensional discrete process generated by a nonlinear map. The most striking example is the onset of chaos via

[1] Department of Physics, Kyushu University, Fukuoka 812, Japan.

0022-4715/83/0300-0649$03.00/0

successive subharmonic bifurcations which can be described by the quadratic map.[1–7] On the other hand, it is well known that, as far as a strange attractor of a dissipative dynamical system is approximately of two dimension,[8] we obtain a one-dimensional map by taking the returning map on the intersection of the attractor and a transverse surface.[3,9] Thus, one-dimensional maps have been playing an important role in the studies of chaotic behaviors of physical systems.

For successive subharmonic bifurcations leading to the onset of chaos, Feigenbaum accomplished a procedure of renormalization of a one-dimensional map,[1,10] and found universal quantities associated with the onset.[11] Since then, many efforts have been devoted to discovering new universal relations for such transitions on the chaos side.[12–17] However, most of them remain phenomenological. Therefore, it would be worthwhile to take a simple model and develop a rigorous and analytic theory of critical phenomena on the chaos side.

In many systems, the degradation of chaos occurs through successive band-splitting transitions as the controlled parameter approaches the onset value of the chaos side. This may be considered as a mirror image of the successive subharmonic bifurcations so that the universality also holds here. Let us take a simple system generated by the following map:

$$g(x;\alpha) = \begin{cases} \alpha x & \text{if} \quad 0 \leqslant x \leqslant 1/2 \\ -\alpha x + \alpha & \text{if} \quad 1/2 < x \leqslant 1 \end{cases} \tag{1.1}$$

The Lyapunov exponent of this map is

$$\lambda(\alpha) = \ln \alpha \tag{1.2}$$

Successive band-splitting transitions occur as the slope α is decreased from two to one.[16,17] It will be shown that a complete procedure of renormalization can be done for this map, and some universal properties can be derived by exact calculation. It must be remarked, however, that the onset of chaos occurs abruptly at the critical value $\alpha = 1$ without successive subharmonic bifurcations. In this paper, our discussion will be concentrated on the band-splitting transitions and on a local structure of the successive band splittings. A global structure will be discussed elsewhere.[18]

One-dimensional maps have been studied extensively by mathematicians.[19–22] Their interest is mostly directed to the topological entropy, the Kolmogorov–Sinai entropy, the topological pressure, and the Artine–Mazur–Ruelle ζ function.[16,23] These quantities offer important information for understanding chaos. They are, however, insensitive to chaos–chaos transitions such as the band splittings, and not useful for the present purpose. On the other hand, the time-correlation functions play the most important role for analyzing time-dependent phenomena in statistical physics,[24] and experimental observations of chaos are usually made on the

power spectra.[3–7] In fact the importance of the theoretical study of time-correlation functions has been emphasized by physicists recently.[25–27]

A qualitative change of chaos by a band-splitting transition is the fact that the strong mixing property is lost so that a persistent oscillation appears in the time-correlation functions. Then, however, the topologically invariant quantities, such as the Lyapunov exponent (1.2), do not exhibit any anomalous behavior.[16] The undamped oscillation gradually arises in such a way that the damping of a critical mode decreases and vanishes at the critical point. This critical slowing-down is a remarkable universal property of band-splitting transitions.[29]

In this paper, therefore, we shall study the asymptotic behavior of the time-correlation function of the map (1.1) near a band-splitting transition point by carrying out an exact calculation for an infinite set of values of the controlled parameter α in order to obtain an analytic expression for the time-correlation function. This will be done by using a new method proposed in a previous paper,[27] namely, by writing the time-correlation function in terms of the Frobenius–Perron operator $\mathscr{H}$ and seeking relevant eigenvalues and eigenfunctions of $\mathscr{H}$. In Section 2, we review the order relation of unstable periodic orbits of the map, which describes the degree of evolution of chaos. We then take two sequences of values of the controlled parameter α, which accumulate to the first band-splitting transition point $\alpha = \sqrt{2}$. In the first half of Section 3, we review the time-correlation functions in terms of the Frobenious–Perron operator $\mathscr{H}$, and discuss a matrix representation of $\mathscr{H}$. In the last half, the time-correlation function of orbits is formulated for the two sequences of α in terms of eigenvalues and eigenfunctions of $\mathscr{H}$. In Section 4, we study the asymptotic behavior of the time-correlation function near the band-splitting transition point. In Section 5, results of numerical calculation are reported for the maps with α being taken arbitrary, and compared with the analytic form for particular α's. In Section 6, we discuss an asymptotic form for a map with asymmetric slopes and conclude with a short summary.

2. EVOLUTION OF CHAOS

Whenever a continuous map f has a nonperiodic orbit, f also has numerous unstable periodic orbits. These periodic orbits have an order relation with respect to their existence, i.e., the Sarkovskii order[30]

$$\begin{aligned} &3|-5|-7|-\cdots|-2\times 3|-2\times 5|-2\times 7|-\cdots \\ &\quad\cdots|-2^n\times 3|-2^n\times 5|-2^n\times 7|-\cdots \\ &\quad\cdots|-2^n|-\cdots|-8|-4|-2|-1 \end{aligned} \tag{2.1}$$

where the first two lines consist of the ascending sequences of $2^n \times M$, $(M = 2m + 1)$ with $n = 0, 1, 2, \ldots,$ and the last line is the descending

powers of 2. This sequence of positive integers indicates that, if f has a periodic orbit of period p, then f also has a periodic orbit of period q for every q which lies on the right-hand side of p in (2.1).

For a one-humped continuous map f,[21] a more severe relation holds in terms of the topological entropy[2] associated with a type of a periodic orbit. Let τ and τ' denote two types of periodic orbits. If the map f has the periodic orbit of τ with $\eta(\tau) > \eta(\tau')$, then f also has the periodic orbit of τ'. With the aid of the map (1.1) with $\alpha = 2$, the new order may read as follows: if a continuous map f has a periodic orbit of type τ, then f has a periodic orbit of type τ' for every type τ' such that the maximum value of the orbit τ' is smaller than that of the orbit τ in the map $g(x; \alpha = 2)$. See Fig. 1.

Let us return to our map (1.1). A periodic orbit of odd period $M = 2m + 1$ exists if and only if $\alpha \geqslant \alpha_M$, where α_M is the positive root of

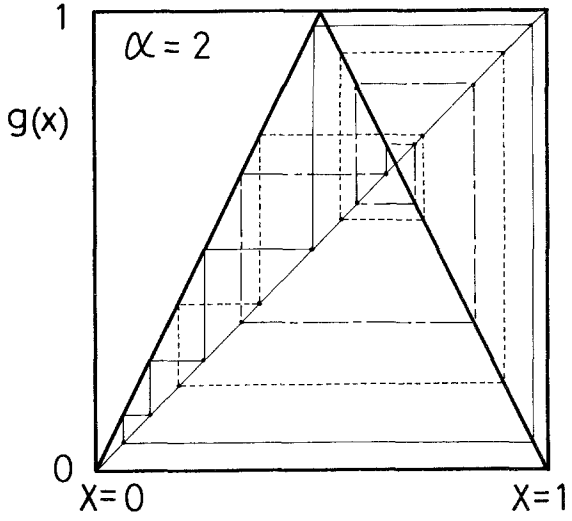

(a)

[2] The topological entropy of f is given by

$$h_{\text{top}}(f) = \lim_{n\to\infty} \frac{1}{n} \log l(f^{(n)})$$

where $f^{(n)}$ is the nth iterate of f and $l(f)$ is the minimum number of intervals necessary for dividing the whole interval into small intervals on each of which f is monotone and continuous. On the other hand, $\eta(\tau)$ is the topological entropy of a piecewise linear map which is the polygonal line obtained by connecting every point of a periodic orbit τ by straight lines in order.

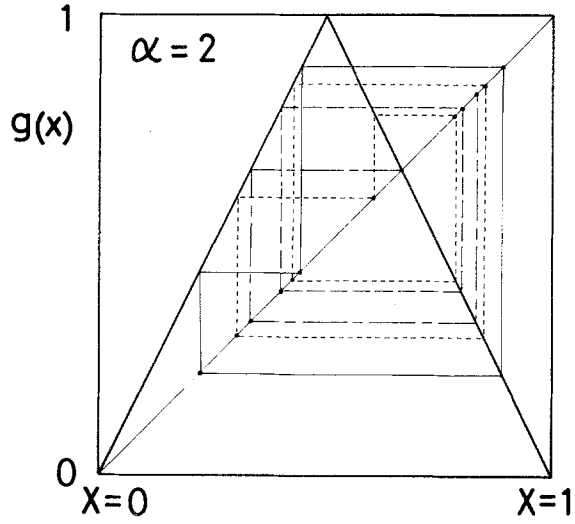

(b)

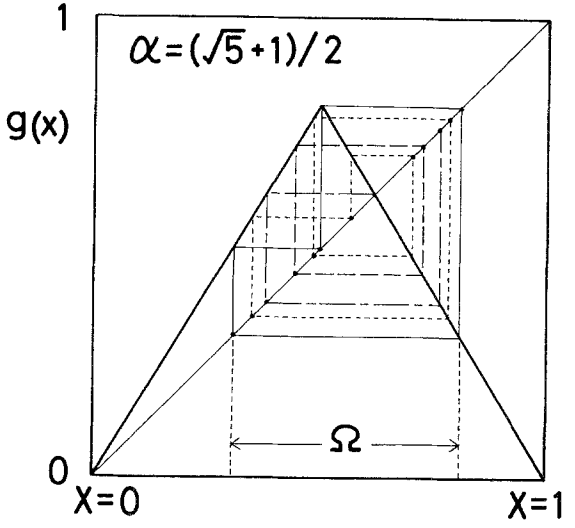

(c)

Fig. 1. Periodic orbits of the map $g(x; \alpha)$ given by (1.1). (a) Three types of period-5 orbits in the case $\alpha = 2$ are shown. The full and dot-dashed lines represent the maximal and minimal orbits, respectively. (b) Minimal orbits of periods 3, 5, and 2 are shown in the case $\alpha = 2$. The periodic orbit of period 5 has the same topological entropy as the minimal orbit of (a). Thus, there are two different orbits for each type of periodic orbits. The dot-dashed line represents an orbit which falls into the fixed point $x = \alpha/(1 + \alpha)$. All orbits of odd periods must go through the outside of this orbit. Hence, as this orbit passes the vertex, all odd periods disappear. (c) The minimal orbits of periods 3, 5, and 2 are shown in the case $\alpha = (\sqrt{5} + 1)/2$. The relative configuration of the orbits is the same as that of (b). Ω denotes the attractor.

the algebraic equation

$$\alpha_M^{2m+1} - 2\alpha_M^{2m-1} - 1 = 0 \qquad \left(2 > \alpha_M > \sqrt{2}\right) \tag{2.2}$$

where $\alpha_M > \alpha_{M+2} > \alpha_\infty = \sqrt{2}$. Therefore, all periods exist if $\alpha \geqslant \alpha_3 = (1+\sqrt{5})/2 = 1.618$. As α is decreased to $\alpha_\infty = \sqrt{2}$, however, odd periods disappear successively in the Sarkovskii order and all odd periods disappear at $\alpha = \sqrt{2}$, where the attractor splits into two bands. This is the mechanism of the band-splitting transition.

Below $\alpha = \sqrt{2}$, each of the two bands repeats the above process in the map $g^{(2)}(x)$ with slope α^2 and splits into two bands at $\alpha^2 = \sqrt{2}$. Thus it turns out that period $2^n \times M$ disappears below

$$\alpha = \alpha_{n:M} = (\alpha_M)^{1/N} \qquad (N \equiv 2^n) \tag{2.3}$$

and the attractor splits into $2N$ bands at $\alpha = \alpha_{n:\infty} = 2^{1/2N}$. All periods disappear at $\alpha = \alpha_{\infty:\infty} = 1$ where chaos disappears.

In order to study the long-time behavior near the first band-splitting transition point $\alpha = \sqrt{2}$, we take two sequences of α's accumulating on $\sqrt{2}$. One is the sequence $\{\alpha_{2m+1}\}$ $(m = 1, 2, \ldots)$. At $\alpha = \alpha_{2m+1}$ the vertex of g lies on the minimal orbit of period $2m+1$. The other sequence consists of α's less than $\sqrt{2}$, at which the maximal orbits[3] of $g^{(2)}$ in each band appear successively with periods $2(m+2)$, as $\alpha \uparrow \sqrt{2}$. Namely, the maximal orbit of period $N = 2(m+2)$ exists in the map $g^{(2)}$ if and only if $\alpha \geqslant \alpha_N$ where

$$\alpha_N^{2(m+2)} - 2\alpha_N^{2(m+1)} + 1 = 0 \qquad \left(\sqrt{2} > \alpha_N > \sqrt[4]{2}\right) \tag{2.4}$$

At $\alpha = \alpha_N$ the maximal orbit of period $2(m+2)$ passes through the vertex of g. For these sequences, exact calculation of the time-correlation function of orbits can be done with a little effort. It is, however, very hard to do it when α falls into a value where the vertex of g lies on a nonperiodic orbit. In such cases, numerical calculation has been done and will be reported in Section 5. It turns out that the analytical results are consistent with the numerical ones.

3. TIME-CORRELATION FUNCTIONS IN TERMS OF $\mathscr{H}$

Let us consider a one-humped continuous map $f(x)$ which has no stable periodic orbit. Namely, f is ergodic on an attractor Ω.[21] Then there

[3] A minimal orbit of period m is the periodic orbit whose topological entropy takes the minimum value among periodic orbits of period m. Similarly, a maximal orbit of period n corresponds to that with the maximum topological entropy among periodic orbits of the same period.

exists a unique absolutely continuous invariant measure[4] $\mu_f^*(dx) = P_f^*(x)\,dx$ so that the long-time average can be replaced by the space average over Ω with the invariant density $P_f^*(x)$.[31] For almost all initial values x, the time-correlation functions takes the form

$$C_k(A,B) \equiv \lim_{N\to\infty} \frac{1}{N} \sum_{n=0}^{N-1} A\big(f^{(n+k)}(x)\big) B\big(f^{(n)}(x)\big) \tag{3.1}$$

$$= \int_\Omega A\big(f^{(k)}(x)\big) B(x) \mu_f^*(dx) \equiv \big\langle \mathscr{L}_f^k A(x) \,|\, B(x) \big\rangle_f \tag{3.2}$$

where $\mathscr{L}_f$ indicates the time-evolution operator defined by[26]

$$\mathscr{L}_f A(x) \equiv A\big(f(x)\big) \tag{3.3}$$

The Frobenius–Perron operator $\mathscr{H}_f$ is the adjoint operator of $\mathscr{L}_f$. Let μ_0 be the usual Lebesgue measure. Then, we have[27]

$$\big\langle \mathscr{L}_f A(x) \,|\, B(x) \big\rangle_f = \int_\Omega dy\, A(y) \int_\Omega \delta\big(y - f(x)\big) B(x) P_f^*(x)\,dx$$

$$= \big\langle A(x) \,|\, \mathscr{H}_f \{B(x) P_f^*(x)\} \big\rangle_0 \tag{3.4}$$

with

$$\mathscr{H}_f G(x) \equiv \int_\Omega dy\, \delta\big(x - f(y)\big) G(y) \tag{3.5}$$

$$= \sum_{y_i\,:\, f(y_i) = x} \frac{1}{|f'(y_i)|} G(y_i) \tag{3.6}$$

It is obvious that the invariant density $P_f^*(x)$ is the eigenfunction of $\mathscr{H}_f$ with eigenvalue unity:

$$\mathscr{H}_f P_f^*(x) = P_f^*(x) \tag{3.7}$$

Therefore, the time-correlation function (3.2) can be transformed into

$$C_n(A,B) = \big\langle A(x) \,|\, \mathscr{H}_f^n \{B(x) P_f^*(x)\} \big\rangle_0 \tag{3.8}$$

This can be calculated exactly if one can find all relevant eigenfunctions of $\mathscr{H}_f$ explicitly.

For the map (1.1), the attractor is located in the interval $[\alpha(1 - \alpha/2), \alpha/2]$. Let us change the coordinate x by a scale transformation so that the interval is transformed into $[0, 1]$. Then, the map g is transformed into

$$f(x) = \begin{cases} \alpha x + 2 - \alpha & \text{if } 0 \leqslant x \leqslant 1 - 1/\alpha \\ -\alpha x + \alpha & \text{if } 1 - 1/\alpha < x \leqslant 1 \end{cases} \tag{3.9}$$

[4] Here, we also assume that f is a piecewise C^2-function. Then, f has a unique absolutely continuous invariant measure. In fact, the mapping (1.1) is such a function. See Ref. 20.

and we have

$$\langle \mathscr{L}_g^n A(x) \mid B(x) \rangle_g$$

$$= \left\langle \mathscr{L}_f^n A\left(\frac{2\alpha - \alpha^2}{2} + \frac{\alpha^2 - \alpha}{2} x \right) \middle| B\left(\frac{2\alpha - \alpha^2}{2} + \frac{\alpha^2 - \alpha}{2} x \right) \right\rangle_f \tag{3.10}$$

Our calculation will be done for (3.9), since only the autocorrelation function of the deviation $\delta x \equiv x - \langle x \rangle_f$ is calculated, and the normalized one by its initial value does not change by the transformation.

Substituting (3.9) into (3.6), we obtain the simple form

$$\mathscr{H}_f G(x) = \frac{1}{\alpha} G\left(\frac{x}{\alpha} - \frac{2 - \alpha}{\alpha} \right) E(x; 2 - \alpha, 1) + \frac{1}{\alpha} G\left(-\frac{x}{\alpha} + 1 \right) \tag{3.11}$$

where $E(x; a, b)$ denotes the characteristic function of the interval $[a, b]$; namely, 1 if $x \in [a, b]$ and 0 otherwise. We find in (3.11) that a continuous function $G(x)$ which has $G(0) \neq 0$ is transformed into a function which is discontinuous at $x = 2 - \alpha$ by $G(0)/\alpha$. Therefore, a repeated operation of $\mathscr{H}_f$ produces a highly discontinous function. The new appearance of discontinuity points finally stops if the discontinuity points cover a closed orbit, such as a periodic orbit, a fixed point, and an orbit falling into them. Then, we have a subspace X_j of the function space $L^2[0, 1]$ such that $\mathscr{H}_f u_j \in X_j$ for every $u_j \in X_j$ and the dimension of X_j is finite. X_j is equivalent, namely isomorphic, to a vector space with the same dimension, where $\mathscr{H}_f$ corresponds to square matrices. For calculation of the time-correlation functions, relevant functions are only those having the same discontinuity points as the invariant density $P_f^*(x)$. These points are identical to the boundary orbit with initial value $x_0 = 1$. Thus, the time-correlation functions can be exactly calculated by use of vector analysis, if the controlled parameter α gives a closed boundary orbit. Such examples are given in the following.

Let us start to calculate the autocorrelation functions of x for the two sequence of α's mentioned in Section 2. For simplicity, henceforward, the first sequence of α's will be referred to as Case (I), and the second as Case (II). According to the illustration of Fig. 2, the interval I is divided into N intervals $\mathrm{I}_1, \mathrm{I}_2, \ldots, \mathrm{I}_N$. Let the jth element of N-dimensional column vectors $\mathbf{a}$ and $\mathbf{b}$ denote the coefficient of x and the constant term on the jth interval I_j, respectively. Therefore, the first-order function of x is represented by the vector form $\mathbf{a}x + \mathbf{b}$.

The Frobenius–Perron operator $\mathscr{H}_f$ can be written as

$$\mathscr{H}_f(\mathbf{a}x + \mathbf{b}) = (\mathscr{H}_1 \mathbf{a})x + (\mathscr{H}_0 \mathbf{b}) + (\mathscr{H}_{\text{in}} \mathbf{a}) \tag{3.12}$$

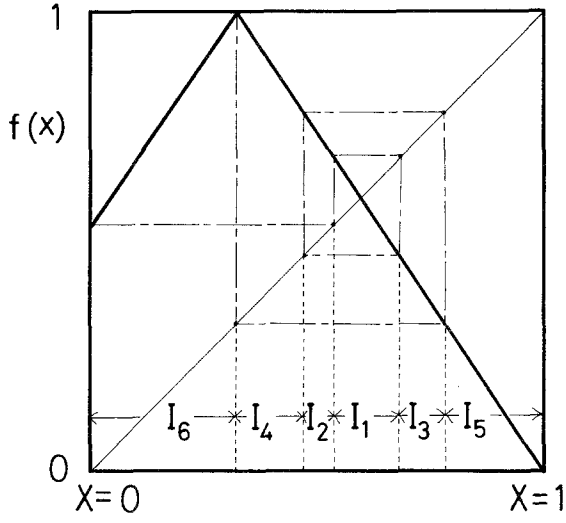

(a)

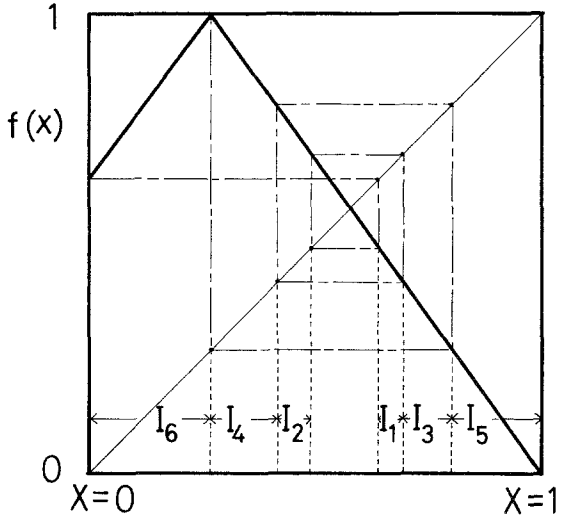

(b)

Fig. 2. The map $f(x;\alpha)$ for two values of α. In (a), α is α_M of (2.2) with $M = 7$, and, in (b), α_N of (2.4) with $N = 8$. I_j is the jth interval of (A.1), ($j = 1, 2, \ldots, 6$).

where $\mathscr{H}_0$, $\mathscr{H}_1$ and $\mathscr{H}_{\text{in}}$ are the $N \times N$ matrices defined by

$$\mathscr{H}_\sigma \equiv \frac{1}{\alpha^{\sigma+1}} \begin{bmatrix} (-1)^\sigma & 0 & 0 & & & & 1 \\ (-1)^\sigma & 0 & 0 & & & & 0 \\ 0 & (-1)^\sigma & 0 & & & & 1 \\ & & & \ddots & & & \vdots \\ & & & & 0 & 0 & 0 \\ & & & & (-1)^\sigma & 0 & 1 \\ & & & & 0 & (-1)^\sigma & 0 \end{bmatrix}$$

for Case (I) (3.13a)

$$\mathscr{H}_\sigma \equiv \frac{1}{\alpha^{\sigma+1}} \begin{bmatrix} 0 & 0 & 0 & & & & 1 \\ (-1)^\sigma & 0 & 0 & & & & 0 \\ 0 & (-1)^\sigma & 0 & & & & 1 \\ & & & \ddots & & & \vdots \\ & & & & 0 & 0 & 0 \\ & & & & (-1)^\sigma & 0 & 1 \\ & & & & 0 & (-1)^\sigma & 0 \end{bmatrix}$$

for Case (II) (3.13b)

$$\mathscr{H}_{\text{in}} \equiv \left(1 - \frac{1}{\alpha}\right)\mathscr{H}_0 - \mathscr{H}_1 \qquad \text{for Case (I) and (II)} \tag{3.14}$$

where $\sigma = 0, 1$. It should be noted that (3.13) is still valid even if $\mathscr{H}_\sigma$ operates on the coefficient vector of the x^σ-term. The kth eigenvalue of $\mathscr{H}_0$ is indicated by (s_k/α). Let $\mathbf{b}_k$ and $\mathbf{b}_k^*$ be its right and left eigenvectors:

$$\mathscr{H}_0 \mathbf{b}_k = \left(\frac{s_k}{\alpha}\right)\mathbf{b}_k, \qquad \mathbf{b}_k^* \mathscr{H}_0 = \mathbf{b}_k^* \left(\frac{s_k}{\alpha}\right) \tag{3.15}$$

Using similar notations for $\mathscr{H}_1$, we have

$$\mathscr{H}_1 \mathbf{a}_k = \left(\frac{t_k}{\alpha^2}\right)\mathbf{a}_k, \qquad \mathbf{a}_k^* \mathscr{H}_1 = \mathbf{a}_k^* \left(\frac{t_k}{\alpha^2}\right) \tag{3.16}$$

The scaled eigenvalues, s_k and t_k, satisfy the eigenvalue equations

$$s^{2m+1} - 2s^{2m-1} - 1 = 0 \qquad \text{with} \quad s \neq -1 \quad \text{for Case (I)} \tag{3.17a}$$

$$s^{2(m+2)} - 2s^{2(m+1)} + 1 = 0 \qquad \text{with} \quad s \neq \pm 1 \quad \text{for Case (II)} \tag{3.17b}$$

and

$$t^{2m+1} - 1 = 0 \qquad \text{with} \quad t \neq \pm 1 \quad \text{for Case (I)} \tag{3.18a}$$

$$t^{2(m+2)} - 1 = 0 \qquad \text{with} \quad t \neq \pm 1 \quad \text{for Case (II)} \tag{3.18b}$$

respectively. Since the boundary conditions, (2.2) and (2.4), are equivalent to (3.17), unity is the maximum eigenvalue of $\mathscr{H}_0$ with $s_1 = \alpha$. Therefore, $\mathbf{b}_1$ gives the invariant density $P_f^*(x)$. (3.17) also has a negative root such that $1 \leqslant |s| \to \alpha$ as $m \to \infty$ for Case (I), and $s = -\alpha$ for Case (II). This eigenvalue plays the central role in the band-splitting transition, and is denoted by s_2. The others give the remained eigenvalues of $\mathscr{H}_0$ whose absolute values tend to $1/\alpha$ as $m \to \infty$. The asymptotic behavior of s_k will be discussed in Section 4. The eigenvectors, $\mathbf{b}_k$, $\mathbf{b}_k^*$, $\mathbf{a}_k$, and $\mathbf{a}_k^*$ are given in Appendix together with other quantities appearing in the course of our calculation. Since a homogeneous function of x is mapped to an inhomogeneous function by $\mathscr{H}_f$ as implied by (3.12), eigenfunctions of $\mathscr{H}_f$ for a polynomial of the first degree take the form

$$\mathbf{x}_k \equiv \mathbf{a}_k x + \sum_{l=1}^{N} \mathbf{b}_l \beta_{lk} \tag{3.19}$$

The coefficients β_{lk} are determined under the condition

$$\mathscr{H}_f \mathbf{x}_k = \left(\frac{t_k}{\alpha^2} \right) \mathbf{x}_k \tag{3.20}$$

with (3.12)–(3.16). It is noted that no pair among the eigenvalues of $\mathscr{H}_0$ and $\mathscr{H}_1$ take an identical value. Of course, this situation is not universal, and breaks down, for example, when the boundary orbit is a closed orbit other than a periodic orbit; see (4.12). Thus we have

$$\beta_{lk} = \frac{\alpha^2}{t_k - \alpha s_l} (\mathbf{b}_l^* \cdot \mathscr{H}_{\text{in}} \mathbf{a}_k) = \frac{(\alpha - 1)s_l - t_k}{t_k - \alpha s_l} (\mathbf{b}_l^* \cdot \mathbf{a}_k) \tag{3.21}$$

The set $\{\mathbf{a}_k, \mathbf{a}_k^*\}$ gives an orthonormal base of the N-dimensional vector space, as well as $\{\mathbf{b}_k, \mathbf{b}_k^*\}$. Under the vector representation of $P_f^*(x)$, therefore, we can write

$$xP_f^*(x) \Rightarrow \mathbf{b}_1 x = \sum_{k=1}^{N} \left[\mathbf{x}_k - \sum_{l=1}^{N} \mathbf{b}_l \beta_{lk} \right] (\mathbf{a}_k^* \cdot \mathbf{b}_1) \tag{3.22}$$

$$\mathscr{H}_f^n x P_f^*(x) \Rightarrow \sum_{k=1}^{N} \left\{ \left(\frac{t_k}{\alpha^2} \right)^n \mathbf{x}_k - \sum_{l=1}^{N} \left(\frac{s_l}{\alpha} \right)^n \mathbf{b}_l \beta_{lk} \right\} (\mathbf{a}_k^* \cdot \mathbf{b}_1) \tag{3.23}$$

Next we have to integrate these quantities over the interval I with an appropriate weight. Let us introduce N-dimensional row vectors $\mathbf{c}_k^*$ whose

jth element $c^*_{k;\,j}$ is given by

$$c^*_{k;\,j} \equiv \int_{I_j} x^k \, dx \tag{3.24}$$

It is obvious that $\mathbf{c}^*_0 = \mathbf{b}^*_1$. Therefore the averages can be written as

$$\langle x \rangle_f = (\mathbf{c}^*_1 \cdot \mathbf{b}_1), \qquad \langle x^2 \rangle_f = (\mathbf{c}^*_2 \cdot \mathbf{b}_1) \tag{3.25}$$

and the time-correlation function takes the form

$$C_n(x,x) = \sum_{k=1}^{N} \left(\frac{t_k}{\alpha^2} \right)^n \left\{ (\mathbf{c}^*_2 \cdot \mathbf{a}_k) + \sum_{l=1}^{N} (\mathbf{c}^*_1 \cdot \mathbf{b}_l)\beta_{lk} \right\} (\mathbf{a}^*_k \cdot \mathbf{b}_1)$$
$$- \sum_{l=1}^{N} \left(\frac{s_l}{\alpha} \right)^n (\mathbf{c}^*_1 \cdot \mathbf{b}_l) \left\{ \sum_{k=1}^{N} \beta_{lk} (\mathbf{a}^*_k \cdot \mathbf{b}_1) \right\} \tag{3.26}$$

The details of this calculation are given in Appendix. For $\beta_{1k} = -(\mathbf{c}^*_1 \cdot \mathbf{a}_k)$, as shown in (A.15), the s_1 term in the last summation of (3.26) is equal to $-\langle x \rangle_f^2$. Finally we find the following expression for the normalized auto-correlation function of $\delta x \equiv x - \langle x \rangle_f$:

$$\xi_n(\alpha) \equiv C_n(\delta x, \delta x) / C_0(\delta x, \delta x) \tag{3.27}$$

$$= \left(\frac{s_2}{\alpha} \right)^n B_2(\alpha) + \sum_{l=3}^{N} \left(\frac{s_l}{\alpha} \right)^n B_l(\alpha) + \sum_{l=1}^{N} \left(\frac{t_l}{\alpha^2} \right) A_l(\alpha) \tag{3.28}$$

where

$$B_l(\alpha) \equiv \frac{2(\alpha^2 - 1)^2 \left[4 + (\alpha^2 - 2)N^* \right]}{9 - 2\alpha + 2\alpha^3 - \alpha^4 + 2(\alpha^2 - 2)N^*}$$
$$\times \frac{s_l (s_l - 1)^2 (s_l + 1)}{(\alpha^2 + s_l)(s_l^2 + \alpha^2 - 2)\left[4 + (s_l^2 - 2)N^* \right]} \qquad (2 \leqslant l \leqslant N) \tag{3.29}$$

$$A_l(\alpha) \equiv \frac{2\alpha(\alpha^2 - 1)^2 \left[4 + (\alpha^2 - 2)N^* \right]}{9 - 2\alpha + 2\alpha^3 - \alpha^4 + 2(\alpha^2 - 2)N^*}$$
$$\times \frac{(1 - t_k^2)\left[t_k^2 - 2\alpha^2(\alpha^2 - 2) \right]}{3N^* t_k (\alpha + t_k)(\alpha^3 + t_k)\left[t_k^2 + \alpha^2(\alpha^2 - 2) \right]} \qquad (1 \leqslant l \leqslant N) \tag{3.30}$$

with the period N^* of the boundary orbit:

$$N^* \equiv 2m + 1 = N + 1 \qquad \text{for Case (I)} \tag{3.31a}$$

$$\equiv 2(m + 2) = N + 2 \qquad \text{for Case (II)} \tag{3.31b}$$

As the next section is prepared to discuss the asymptotic behaviors of ξ_n in details, we give a brief comment. For $\sqrt{2} > \alpha > \sqrt[4]{2}$, $s_2 = -\alpha$ so that the first term of (3.28) describes the undamped oscillation of period 2, and its amplitude B_2 remains finite in the limit $\alpha \uparrow \sqrt{2}$. But the other modes damp and their amplitudes vanish as $O(1/N^*)$ in this limit. As $\alpha \downarrow \sqrt{2}$, $s_2 \downarrow -\alpha$ so that the critical mode damps but slightly, while the other situations mentioned above are fundamentally invariant. Finally, let us examine the simplest cases, namely, $m = 1$. Then, the boundary orbit has period 3 for Case (I), or period 2×3 for Case (II). Their eigenvalues are given by

$$s_{\{\frac{1}{2}\}} = \frac{1}{2}(1 \pm \sqrt{5}), \qquad t_1 = t_2^\dagger = \exp\left(\frac{2\pi}{3} i\right) \qquad \text{for Case (I)} \tag{3.32a}$$

$$\left.\begin{aligned} s_{\{\frac{1}{2}\}} &= \pm\left(\frac{\sqrt{5}+1}{2}\right)^{1/2}, \qquad s_3 = s_4^\dagger = i\left(\frac{\sqrt{5}-1}{2}\right)^{1/2} \\ t_1 &= t_2^\dagger = \exp\left(\frac{\pi}{3} i\right), \qquad t_3 = t_4^\dagger = \exp\left(\frac{2\pi}{3} i\right) \end{aligned}\right\} \quad \text{for Case (II)} \tag{3.32b}$$

where $a^\dagger$ denotes the complex conjugate of a. Substituting these values into (3.28), (3.29), and (3.30), and taking into account $\alpha = s_1$, we obtain

$$\xi_n(\alpha) = \left(-\frac{1}{\alpha^2}\right)^n - \frac{2\sqrt{15}}{9}\left(\frac{1}{\alpha^2}\right)^n \sin\left(\frac{2\pi}{3} n\right) \qquad \text{at} \quad \alpha = \frac{\sqrt{5}+1}{2} \tag{3.33a}$$

$$\begin{aligned} \xi_n(\alpha) = {} & 0.9466 \times (-1)^n + 0.0535 \\ & \times \left(\frac{1}{\alpha^2}\right)^n \left[\cos\frac{\pi}{2} n - \frac{\sqrt{15}}{9}\left(\sin\frac{\pi}{3} n - \sin\frac{2\pi}{3} n\right)\right] \\ & - 0.0260 \times \left(\frac{1}{\alpha^2}\right)^n \left[\sin\frac{\pi}{2} n + \frac{5\sqrt{3}}{18}\left(\sin\frac{\pi}{3} n + \sin\frac{2\pi}{3} n\right)\right. \\ & \left. - \frac{\sqrt{5}}{6}\left(\cos\frac{\pi}{3} n - \cos\frac{2\pi}{3} n\right)\right] \\ & \text{at} \quad \alpha^2 = \frac{\sqrt{5}+1}{2} \end{aligned} \tag{3.33b}$$

Equation (3.33a) agrees with that obtained previously.[27] We find that the second term of (3.33b) agrees with that obtained by rescaling the time scale

of (3.33a) twice. This agreement represents the renormalizability of $f^{(2)}$ of $\alpha = \sqrt{\alpha_3}$ to f of $\alpha = \alpha_3$, where $\alpha_3 = (\sqrt{5} + 1)/2$.[1] Odd times iterated maps of f of $\alpha = \sqrt{\alpha_3}$, however, are not renormalizable to f of $\alpha = \alpha_3$. The last term of (3.33b) cannot be transformed to (3.33a). Therefore, the complete renormalizability to (3.33a) in the power spectrum breaks down. A detailed discussion of the renormalization in this successive transition is given elsewhere.[18]

4. ASYMPTOTIC BEHAVIORS OF ξ_n NEAR THE CRITICAL POINT $\alpha = \sqrt{2}$

We first discuss the asymptotic behaviors of ξ_n as α approaches $\sqrt{2}$. Then ξ_n at $\alpha = \sqrt{2}$ is calculated independently, and compared with the asymptotic one, since the critical point $\sqrt{2}$ is not contained in our sequences.

Let us return to the eigenvalue equations (3.17):

$$s_k^2 = 2 + \left(\frac{1}{s_k}\right)^{2m-1} \qquad \text{with} \quad s_k \neq 1 \quad \text{for Case (I)} \tag{4.1a}$$

$$s_k^2 + \left(\frac{1}{s_k^2}\right)^{2m+1} = 2 \qquad \text{with} \quad s_k^2 \neq 1 \quad \text{for Case (II)} \tag{4.1b}$$

This relation can be represented by a triangle on the complex plane as shown in Fig. 3. Each term corresponds to each side. Since the absolute value of s_k is restricted by a triangular inequality, we have two real roots, $s_1 = \alpha$ and $1 \leqslant -s_2 \leqslant \alpha$, and $(N-2)$ complex roots such that $|s_k| < 1$. The N is related to period N^* of (3.31), and N^* can be written as

$$N_m^* = 2 - \frac{\ln|\alpha_{(m)}^2 - 2|}{\ln \alpha_{(m)}} \tag{4.2}$$

where $\alpha_{(m)} = \alpha_{2m+1}$ for Case (I) and $\alpha_{2(m+2)}$ for Case (II). Equations (2.2) and (2.4) give for large m

$$\alpha_{(m)} - \sqrt{2} \sim \eta^{-m} \qquad \text{with} \quad \eta = 2 \tag{4.3}$$

This convergence rate η has the same value as the accumulation rate δ of the successive transitions near $\alpha = 1$, reflecting the linearity of the continuous map f. In the single band region, s_2 can be written as

$$s_2 = -\left[2 + \left(\frac{1}{s_2}\right)^{2m-1}\right]^{1/2} \cong -\sqrt{2} + \left(\alpha_{(m)} - \sqrt{2}\right) \tag{4.4}$$

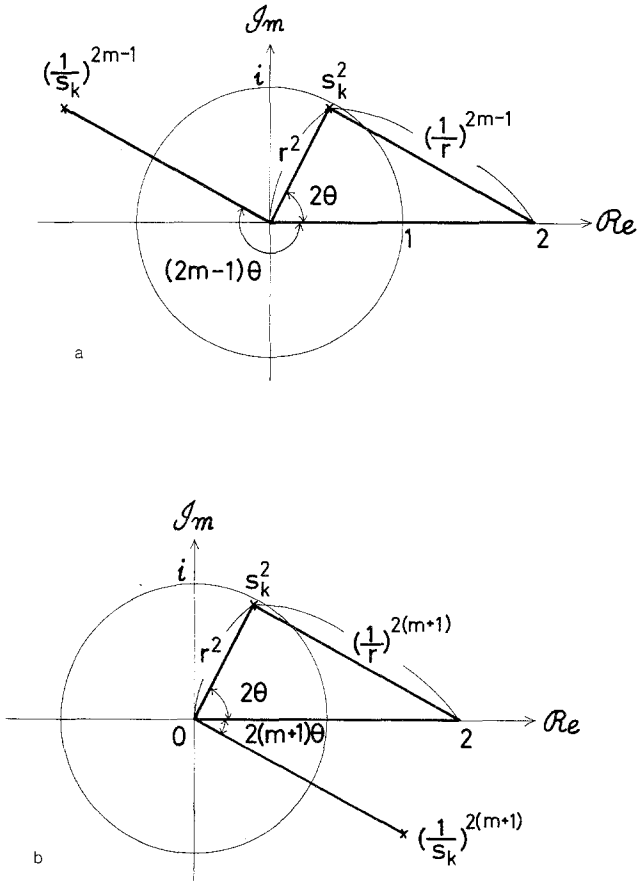

Fig. 3. The triangles represent the relation of (4.1) on the complex plane, where $s_k = r\exp(i\theta)$. (a) is for (4.1a), and (b) for (4.1b). In the limit $m \to \infty$, r^{-2m} can take the null value or a finite value c such that $1 \leqslant c \leqslant 3$. The former limit arises from the two real roots s_1 and s_2. The latter occurs from the remaining $(N-2)$ roots of (4.5).

for large m and goes to $-\sqrt{2}$ with the same convergence rate η as $\alpha \downarrow \sqrt{2}$. The complex roots are given for large m by

$$s_{2k+1} = s_{2k+2} \cong \left(5 - 4\cos\frac{2k}{m}\pi\right)^{-1/4m} \exp\left[i\frac{\pi}{m}(k+\delta_k)\right]$$
$$\text{with} \quad |\delta_k| \leqslant 1 \quad (1 \leqslant k \leqslant m-1) \qquad (4.5)$$

Similarly, in the two-band region, $s_2 = -\alpha$, and the complex roots distribute homogeneously on the unit circle in the limit $\alpha \uparrow \sqrt{2}$.

As $\alpha \to \sqrt{2}$, the amplitude $B_l(\alpha)$ with $l \geqslant 3$ has the limit such that

$$\lim_{\alpha \to \sqrt{2}} N^* B_l(\alpha) = -\frac{8(5-2\sqrt{2})}{17} \frac{(e^{ix}-1)^2(e^{ix}+1)}{e^{ix}(2+e^{ix})(2-e^{2ix})} \tag{4.6}$$

with

$$\lim_{\alpha \to \sqrt{2}} \frac{\pi}{m}(k+\delta_k) \equiv x \tag{4.7}$$

where we have used (4.2). Taking into account the homogeneous distribution of $s_{k \geqslant 3}$ on the unit circle, we can write the second term of (3.28) for large m as

$$\sum_{l=3}^{N} \left(\frac{s_l}{\alpha}\right)^n B_l(\alpha) \cong -\frac{8(5-2\sqrt{2})}{17} \left(\frac{1}{\sqrt{2}}\right)^n \times \frac{1}{2\pi} \int_0^{2\pi} dx\, e^{i(n-1)x} \frac{(e^{ix}-1)^2(e^{ix}+1)}{(2+e^{ix})(2-e^{2ix})} \tag{4.8}$$

This situation is also applicable to the third term of (3.28), since t_k is a complex N^* power root of 1. Then, we have for large m

$$\sum_{l=1}^{N} \left(\frac{t_l}{\alpha^2}\right)^n A_l(\alpha) \cong \frac{8(5\sqrt{2}-4)}{51} \left(\frac{1}{2}\right)^n \times \frac{1}{2\pi} \int_0^{2\pi} dx\, e^{i(n-1)x} \frac{1-e^{2ix}}{(\sqrt{2}+e^{ix})(2\sqrt{2}+e^{ix})} \tag{4.9}$$

The first term of (3.28) takes the asymptotic form for large m,

$$\left(\frac{s_2}{\alpha}\right)^n B_2(\alpha) \cong \frac{7+4\sqrt{2}}{17} (-1)^n \exp\left[-\sqrt{2}(\alpha-\sqrt{2})n\right] \tag{4.10}$$

in the single band region, where (4.3) and (4.4) have been used. In the two-band region (4.10) must be replaced by that without damping.

The integrals of (4.8) and (4.9) can be easily calculated with the help of complex integral. The origin is the only pole which contributes to these integrals for $n = 0$ and 1. There is no pole contributing to them for $n \geqslant 2$. Thus, the contribution to the power spectrum from all damping modes except the critical mode is nearly white. Thus finally we obtain the

asymptotic form

$$\xi_n(\alpha) \cong \frac{10-4\sqrt{2}}{17}\delta_{n,0} - \frac{10\sqrt{2}-8}{51}\delta_{n,1}$$

$$+ \frac{7+4\sqrt{2}}{17}(-1)^n \exp\left[-\sqrt{2}\,(\alpha-\alpha_c^{(1)})n\right] \qquad (\alpha_c^{(1)}=\sqrt{2}) \quad (4.11)$$

in the single band region near the band-splitting transition point $\alpha=\sqrt{2}$.

Equation (4.11) indicates the validity of the gate image which was discussed in a decay of metastable chaos by Yorke and Yorke[32] and applied to band-splitting transitions by Schenker and Kadanoff.[29] It tells that, under f,[2] the mean trapped time of points in one band is proportional to the width of the narrow gate which is the interval mapped out of the band. It appears as the decay time of the third term of (4.11). The first two terms describe the mixing process in the one band, which has a δ-correlation under $f^{(2)}$.

We can show the behavior of ξ_n at $\alpha=\sqrt{2}$. The state functions relevant to ξ_n may be discontinuous at the fixed point or the vertex of $f(x)$. Then, $\mathscr{H}_0$ and $\mathscr{H}_1$ of (3.12) must take the form

$$\mathscr{H}_0 = \frac{1}{\sqrt{2}}\begin{bmatrix}0&0&1\\0&0&1\\1&1&0\end{bmatrix}, \qquad \mathscr{H}_1 = \frac{1}{2}\begin{bmatrix}0&0&-1\\0&0&-1\\1&-1&0\end{bmatrix} \qquad (4.12)$$

where the first, second and third intervals are $[0, 1-1/\sqrt{2}]$, $[1-1/\sqrt{2}, 2-\sqrt{2}]$ and $[2-\sqrt{2}, 1]$, respectively. All eigenvalues of $\mathscr{H}_1$ are 0, while those of $\mathscr{H}_0$ are 1, -1 and 0 whose eigenvectors are

$$\mathbf{b}_1 = \frac{2+\sqrt{2}}{4}\begin{bmatrix}1\\1\\\sqrt{2}\end{bmatrix}, \qquad \mathbf{b}_2 = \frac{2-\sqrt{2}}{4}\begin{bmatrix}1\\1\\-\sqrt{2}\end{bmatrix}, \qquad \mathbf{b}_3 = \frac{1}{2}\begin{bmatrix}1\\-1\\0\end{bmatrix} \quad (4.13)$$

This situation for $\mathscr{H}_1$ leads to $\mathscr{H}_1^3 = 0$, and we have

$$\mathscr{H}_f \mathbf{b}_1 x = -\left(\frac{\sqrt{2}}{4}\mathbf{b}_1 + \frac{3\sqrt{2}+4}{4}\mathbf{b}_2\right)x + \frac{4-\sqrt{2}}{4}\mathbf{b}_1 + \frac{4+3\sqrt{2}}{4}\mathbf{b}_2 \quad (4.14a)$$

$$\mathscr{H}_f^2 \mathbf{b}_1 x = \frac{5-2\sqrt{2}}{4}\mathbf{b}_1 - \frac{3+2\sqrt{2}}{4}\mathbf{b}_2 \quad (4.14b)$$

Then, it is easily shown that

$$C_n(x,x) = \begin{cases} \langle x\rangle_f^2 + \frac{1}{16}(7-4\sqrt{2}) & \text{if } n=0 \\ \langle x\rangle_f^2 + \frac{1}{48}(5-6\sqrt{2}) & \text{if } n=1 \\ \langle x\rangle_f^2 + \frac{1}{16}(-1)^n & \text{if } n \geqslant 2 \end{cases} \tag{4.15}$$

with $\langle x\rangle_f = (5-2\sqrt{2})/4$. This strictly coincides with that of (3.26) as $\alpha = \sqrt{2}$. Therefore, it is obvious that ξ_n at $\alpha = \sqrt{2}$ is given by

$$\xi_n(\sqrt{2}) = \frac{10-4\sqrt{2}}{17}\delta_{n,0} - \frac{10\sqrt{2}-8}{51}\delta_{n,1} + \frac{7+4\sqrt{2}}{17}(-1)^n \tag{4.16}$$

which is just that obtained by substituting $\sqrt{2}$ for α in (4.11).

5. NUMERICAL CALCULATION

We have calculated the time-correlation function of orbits for the two sequences of α. There exists the question whether the behavior of the time-correlation function for these values of α is generic or nongeneric. The answer is given by studying it for α being taken arbitrarily. However, it is very hard to calculate the time-correlation function when α falls into a value where the vertex of f lies on a nonperiodic orbit. Actually it occurs for almost all $\alpha > 1$. In such cases, we have studied the time-correlation function by numerical iteration calculation instead of analytical calculation.

First the numerical calculation of the theoretical formulas presented in the preceding sections has been done for α given in Table I, where α_M for the period-M orbit was determined by (2.2) for some odd numbers M. On the other hand, numerical iteration calculation has been done for α given in Table II, where the noninteger number M of α_M was determined by (4.2). The time-correlation function of orbits is obtained by the direct calculation of (3.1). As an initial value for the iteration calculation of an orbit, an irrational number was used, for example, $x_0 = 0.3127/\sqrt{3}$. The number of iteration steps, N, was 5×10^5 and 2×10^6, and all calculated elements of the orbit, x_n $(n = 0, 1, \ldots)$, were used to calculate the time-correlation function from (3.1). Some typical results of the numerical iteration calculation are shown in Figs. 4–6 for $M = 5.8$, 9.0, and 11.5. Figure 4 shows the normalized time-correlation functions, where the oscillatory behavior lasts longer as M becomes larger. The power spectrum, the Fourier–Laplace transform of (3.1), is shown in Fig. 5. Especially, in Figs. 4b, 5b, and 6, we

Table I. The Linewidth of the Power Spectrum of Orbits with Period-M Vertices Calculated by the Present Theory[a]

M	a_M	$-\ln\lvert s_2/\alpha_M\rvert$	$\sqrt{2}\,(\alpha_M-\sqrt{2}\,)$	γ	$\gamma P_{\max}(\omega)$
3	1.618 034	0.962 424	0.288 246	1.212 355	2.413 450
5	1.512 876	0.249 580	0.139 530	0.286 756	1.276 115
7	1.465 571	0.101 046	0.072 631	0.107 326	0.988 467
9	1.441 315	$4.652\,26\times10^{-2}$	$3.832\,79\times10^{-2}$	$4.797\,21\times10^{-2}$	0.877 601
11	1.428 423	$2.251\,93\times10^{-2}$	$2.009\,48\times10^{-2}$	$2.289\,27\times10^{-2}$	0.820 996
13	1.421 573	$1.112\,24\times10^{-2}$	$1.040\,83\times10^{-2}$	$1.122\,16\times10^{-2}$	0.788 936
21	1.414 699	$6.905\,83\times10^{-4}$	$6.859\,32\times10^{-4}$	$6.910\,42\times10^{-4}$	0.749 157
31	1.414 229	$2.157\,92\times10^{-5}$	$2.157\,23\times10^{-5}$	$2.157\,97\times10^{-5}$	0.744 744
41	1.414 214	$6.743\,50\times10^{-7}$	$6.743\,41\times10^{-7}$	$6.743\,50\times10^{-7}$	0.744 530
51	1.414 2136	$2.107\,34\times10^{-8}$	$2.107\,34\times10^{-8}$	$2.107\,34\times10^{-8}$	0.744 521

[a] α_M and s_2 are the positive and negative roots of (2.2) other than -1, respectively. γ and $P_{\max}(\omega)$ are the half-width at half-height and the peak height of the power spectrum, respectively. As M is increased, $\gamma P_{\max}(\omega)$ reduces to $(7+4\sqrt{2}\,)/17$ as suggested by the third coefficient of (4.11). This fact means that the power spectrum reduces to the Lorentzian with M being increased.

Table II. The Linewidth of the Power Spectrum of Orbits with Periodic and Nonperiodic Vertices Obtained by the Numerical Iteration Calculation with $N = 5 \times 10^5$ [a]

M	α_M	$\sqrt{2}(\alpha_M - \sqrt{2})$	γ	$\gamma P_{\max}(\omega)$
5.8	1.489 896	0.107 031	0.1951	1.1802
9.0	1.441 315	$3.832\,79 \times 10^{-2}$	4.721×10^{-2}	0.8735
9.8	1.435 174	$2.964\,12 \times 10^{-2}$	3.634×10^{-2}	0.8502
11.5	1.426 282	$1.706\,72 \times 10^{-2}$	1.902×10^{-2}	0.8095

[a] The nonintegral number M of α_M is calculated from (4.2). γ and $P_{\max}(\omega)$ are the half-width at half-height and the peak height of the power spectrum, respectively.

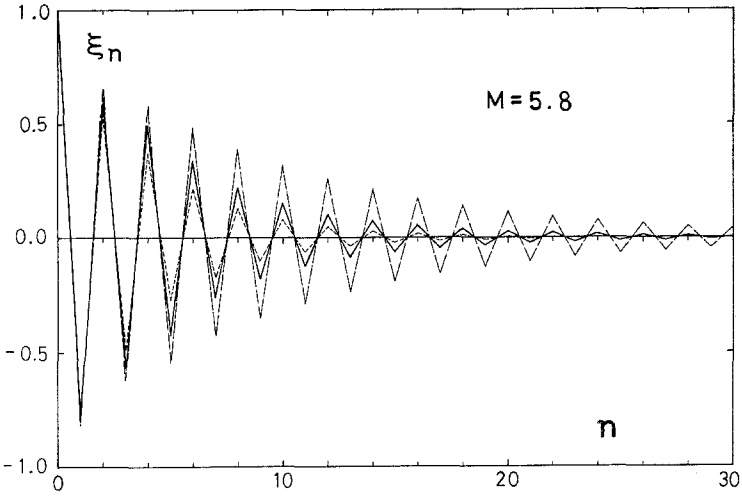

(a)

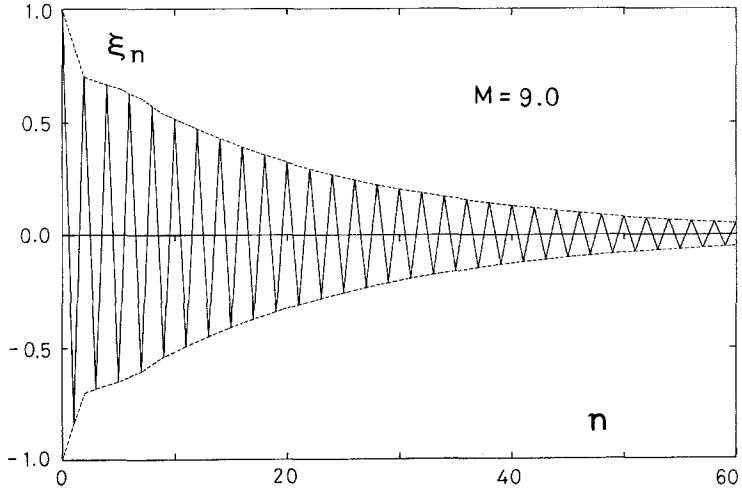

(b)

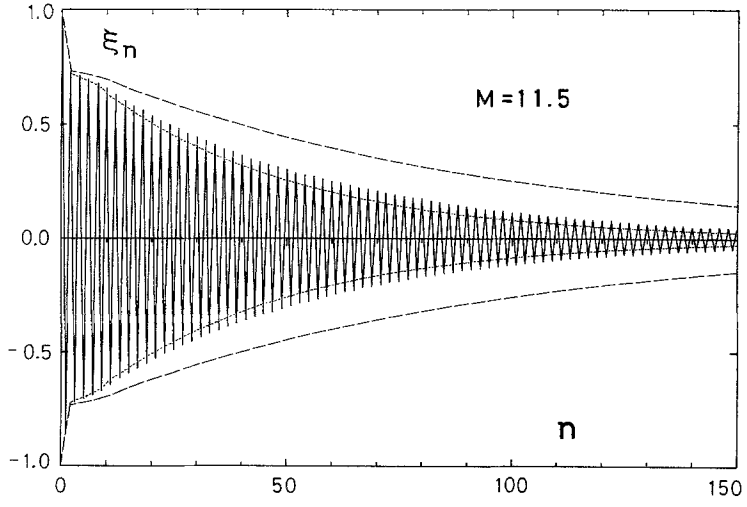

(c)

Fig. 4. The normalized time-correlation function for $M = 5.8$, 9.0 and 11.5 calculated by numerical iteration with $N = 5 \times 10^5$. (a) The dotted and dashed lines show the theoretical time-correlation function for $M = 5$ and 7, respectively, calculated from (3.28)–(3.30). (b) The dotted line shows the envelope of the theoretical time-correlation function for $M = 9$. (c) The dotted and dashed lines show the envelopes of the theoretical time-correlation function for $M = 11$ and 13, respectively.

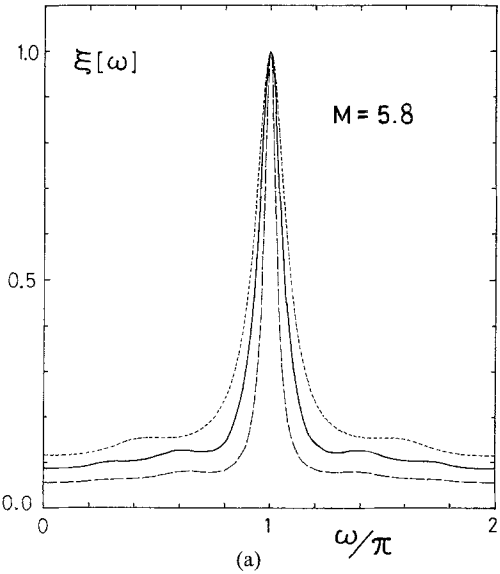

(a)

Fig. 5. The power spectra for $M = 5.8$, 9.0, and 11.5 calculated by numerical iteration with $N = 5 \times 10^5$, which are shown by solid lines in (a), (b), and (c), respectively. All the peak heights of the spectra presented here are normalized to unity. (a) The dotted and dashed lines show the theoretical power spectra for $M = 5$ and 7, respectively. (b) The dotted line shows the theoretical power spectrum for $M = 9$. (c) The dotted and dashed lines show the theoretical power spectra for $M = 11$ and 13, respectively.

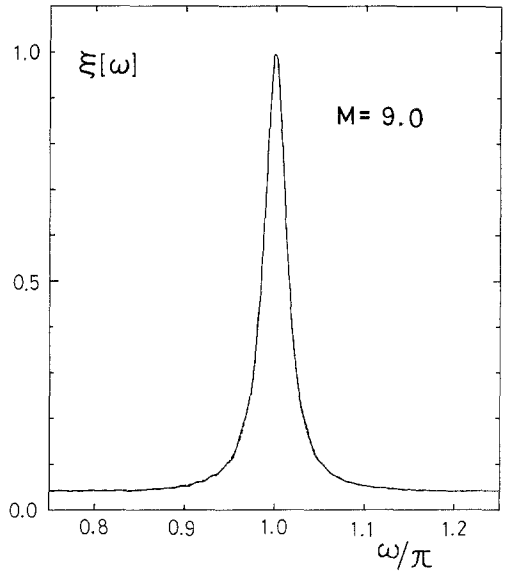
1.0
0.5
0.0
ξ[ω]
M= 9.0
0.8
0.9
1.0
1.1
1.2
ω/π

(b)

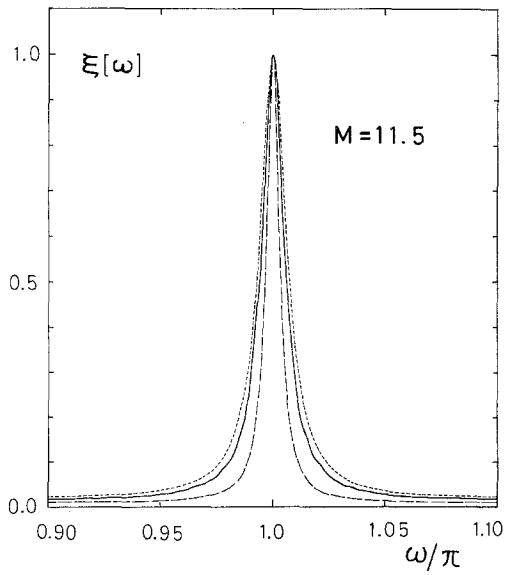
1.0
0.5
0.0
ξ[ω]
M=11.5
0.90
0.95
1.0
1.05
1.10
ω/π

(c)

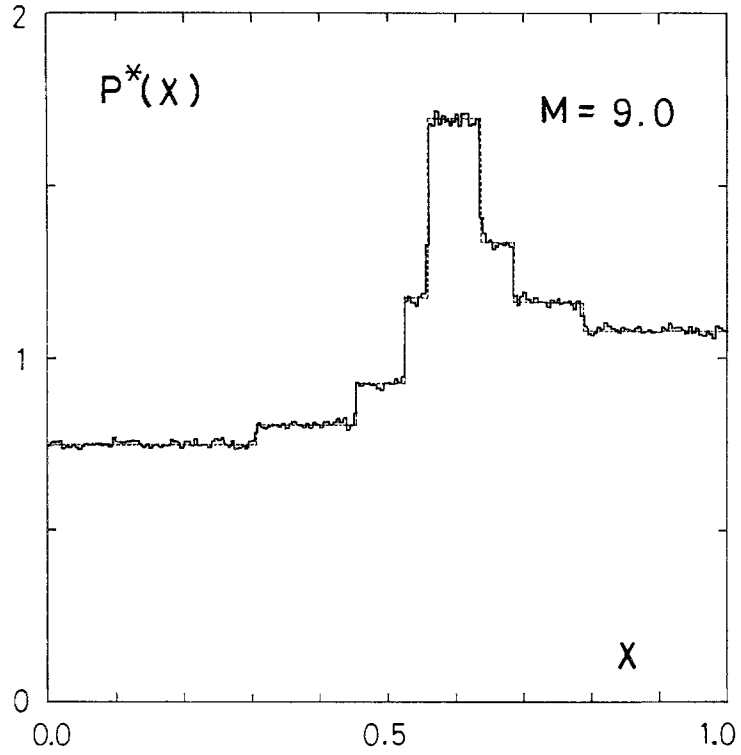

Fig. 6. The invariant density for $M = 9.0$ calculated by numerical iteration with $N = 2 \times 10^6$. The dotted line shows the theoretical invariant density for $M = 9$ calculated from (A.2) and (A.3a).

can find that the present result for $M = 9.0$ by the numerical iteration calculation coincides completely with the theoretical exact analysis. In Fig. 5, the peak of the power spectrum locates at $\omega = \pi$ and the line shape becomes sharper extremely as M is increased and reduces to the Lorentzian line shape, because the intensity of the power spectrum $\gamma P_{\max}(\omega)$ reduces rapidly to the third coefficient of (4.11), i.e., $(7 + 4\sqrt{2})/17 = 0.744\,5208$. The half-linewidth γ at half-height of the power spectrum is shown in Fig. 7 and listed in Table I, together with $-\ln|s_2/\alpha|$ and $\sqrt{2}(\alpha_M - \sqrt{2})$. As M is increased, these values merge into a straight line rapidly, as can be seen in Fig. 7, where γ decreases exponentially with M for $M \geqslant 9$, i.e., $\gamma = 2^{-(M/2)}$. The above results give evidence that the asymptotic expressions (4.4) and (4.10) for the normalized time-correlation function also hold. Thus, it is concluded that the time-correlation function and power spectrum vary continuously with α being varied continuously.

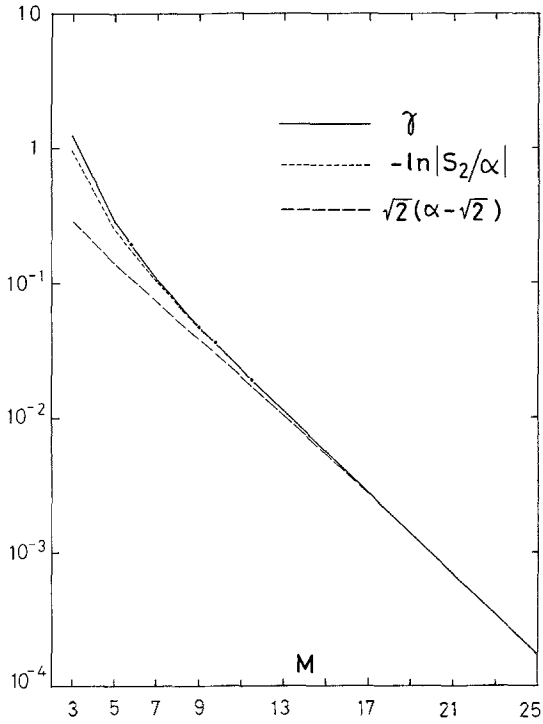

Fig. 7. The half-linewidth at half-height of the theoretical power spectrum, γ is shown by the solid line. The others shown by the dotted and dashed lines are approximate results deduced from the present theory. Those data are tabulated in Table I. The dots show the half-linewidth at half-height of the power spectra obtained by numerical iteration calcualtion tabulated in Table II.

6. SHORT SUMMARY AND SOME REMARKS

We have studied a band-splitting transition in terms of the time-correlation function of orbits of the map (1.1) by taking two sequences of values of α which accumulate to the transition point $\alpha=\sqrt{2}$ from above and below, respectively. We have found that, as α approaches the transition point $\alpha=\sqrt{2}$, two eigenvalues of $\mathscr{H}_f$, the eigenvalues of the invariant measure and the critical mode, are apparently isolated from the others and have the above values equal and nearly equal to unity, respectively. Thus we have derived the asymptotic form (4.11) for the time-correlation function near the transition point. We have also found that the time-correlation function rapidly approaches the asymptotic form. In the limit $\alpha\to\sqrt{2}$, the asymptotic form agrees with the time-correlation function (4.16) at the transition point. Therefore, we find that the asymptotic form of the time-correlation function can simply be obtained from the time-

correlation function at the transition point and the isolated eigenvalues of $\mathscr{H}_f$.

Numerical calculation has also been done for the maps with α being taken arbitrary. It turns out that the analytical results are consistent with the numerical ones. Therefore, it seems that the time-correlation function changes continuously, but not smoothly, with respect to the controled parameter α, as well as other average quantities. The critical region of this band-splitting transition is sufficiently wide and the critical slowing down is easily observable.

The time correlation of orbits of the map (1.1) shows a δ-function-like decay at the transition point. This behavior comes from the symmetry of the slope. For the successive band-splitting transitions of the quadratic map, the iterated map has an asymmetric form in almost every band.[1] In order to study the effect of the asymmetry, let us consider the map

$$h(x) = \begin{cases} \beta x + 1 + \beta/\alpha - \beta & \text{if} \quad 0 \leqslant x \leqslant 1 - 1/\alpha \\ -\alpha x + \alpha & \text{if} \quad 1 - 1/\alpha < x \leqslant 1 \end{cases} \tag{6.1}$$

The map (6.1) has the phase diagram of Fig. 8.[17] The band-splitting to two bands occurs on the critical line

$$\alpha = \alpha_c(\gamma) \equiv (1 + \gamma)^{1/2} \tag{6.2}$$

where $\gamma = \alpha/\beta$. The mechanism of this transition is the same as mentioned in Section 2, while the disappearance of odd period $M = 2m + 1$ occurs on the line $\alpha = \alpha_M(\gamma)$, where

$$\alpha_M^{2m+1} - (1 + \gamma)\alpha_M^{2m-1} - \gamma = 0 \tag{6.3}$$

with $\alpha_M > 1$. The isolated eigenvalues of $\mathscr{H}_f$ are involved in eigenvalues of $\mathscr{H}_0$ whose eigenvalue equation, after being scaled out by α, is equal to (6.3) with $\alpha_M \neq 1$. Therefore, the relevant eigenvalues for the asymptotic form of the time-correlation function can be written for large m as

$$\alpha_M(\gamma) \cong \alpha_c(\gamma) + \frac{1}{2} \frac{\gamma}{[\alpha_c(\gamma)]^{2m}} \tag{6.4}$$

$$s_2(\gamma) \cong -\alpha_c(\gamma) + \frac{1}{2} \frac{\gamma}{[\alpha_c(\gamma)]^{2m}} \cong -\alpha_c(\gamma) + [\alpha_M(\gamma) - \alpha_c(\gamma)] \tag{6.5}$$

The time-correlation function on the critical line (6.2) can be calculated in the similar way to Section 4. The eigenvalues of $\mathscr{H}_1$ are $0, [(1 - \gamma)/(\gamma + 1)]^{1/2}, -[(1 - \gamma)/(\gamma + 1)]^{1/2}$ if $\gamma < 1$, and $0, i[(\gamma - 1)/(\gamma + 1)]^{1/2}, -i[(\gamma - 1)/(\gamma + 1)]^{1/2}$ if $\gamma > 1$, while those of $\mathscr{H}_0$ are the same as in Section 4; namely, $0, 1, -1$. The zero eigenvalue of $\mathscr{H}_0$ and $\mathscr{H}_1$ have no contribution to the time-correlation function. The decay of the time-correlation of orbits is described by the remaining two eigenvalues of $\mathscr{H}_1$.

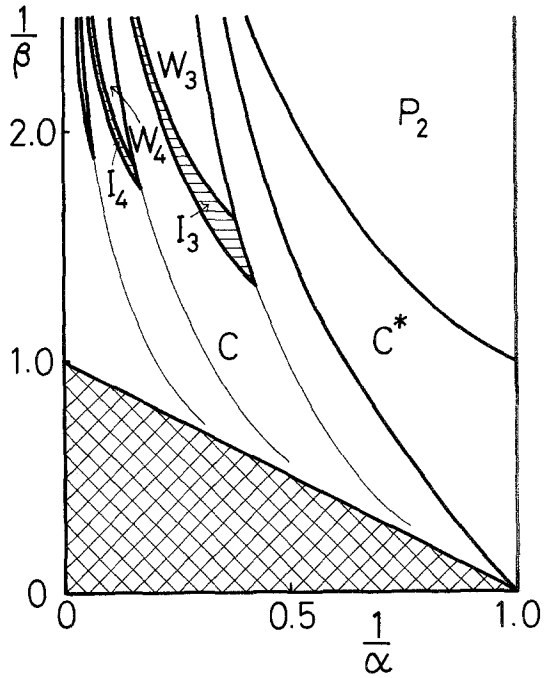

Fig. 8. The phase diagram of the map $h(x; \alpha, \beta)$ given by (6.1). C and C* indicate the regions of chaos with and without the strong mixing, respectively. Successive band-splitting transitions occur in C*. I and W denote the regions called "island" and "window," respectively. P_2 denotes the region of a stable period-2 orbit. In the meshed region, $h(x; \alpha, \beta)$ cannot be constructed. The heavy lines are the phase boundaries, and the light lines in C represent the positions where the maximal orbits of periods 3, 4, and 5 appear.

Then, the time-correlation function takes the form

$$C_n(x,x) = \begin{cases} \langle x\rangle_h^2 + \dfrac{1}{16}(-1)^n + \dfrac{\gamma+2}{48\gamma^2}\left[1 - \dfrac{2(\gamma+1)^{1/2}}{\gamma+2}\right]\left(\dfrac{1-\gamma}{1+\gamma}\right)^{n/2} \\ \qquad \times\left[(\gamma+2)(1+\cos n\pi) - \dfrac{2}{(1-\gamma)^{1/2}}(1-\cos n\pi)\right] \\ \qquad\qquad\qquad\qquad\qquad\qquad\qquad\qquad \text{if} \quad \gamma < 1 \\ \langle x\rangle_h^2 + \dfrac{1}{16}(-1)^n + \dfrac{\gamma+2}{24\gamma^2}\left[1 - \dfrac{2(\gamma+1)^{1/2}}{\gamma+2}\right]\left(\dfrac{\gamma-1}{\gamma+1}\right)^{n/2} \\ \qquad \times\left[(\gamma+2)\cos\dfrac{n\pi}{2} - \dfrac{2}{(\gamma-1)^{1/2}}\sin\dfrac{n\pi}{2}\right] \quad \text{if} \quad \gamma > 1 \end{cases} \tag{6.6}$$

where $\langle x \rangle_h = [3\gamma + 2 - 2(\gamma + 1)^{1/2}]/4\gamma$. The asymptotic form near the transition point is obtained by replacing the second term of (6.6) by

$$\frac{1}{16}\left(\frac{s_2}{\alpha}\right)^n \cong \frac{1}{16}(-1)^n \exp\left\{-\frac{2n}{\alpha_c(\gamma)}[\alpha - \alpha_c(\gamma)]\right\}$$

with fixed γ. As $\gamma \to 1$, (6.6) agrees with (4.15). This would support the assumption that, in the successive band-splitting transition of the quadratic map, the asymmetry of the iterated map does not give any important effect to the time correlation of orbits. However, it must be remarked that the time correlation of orbits is not the δ-correlation given in Ref. 13.[18]

The map (6.1) also has band-splitting transitions which are due to a different mechanism from the map (1.1). They occur on the boundaries between C and I in Fig. 8. Making use of the order relation of periodic orbits in terms of the topological entropy, we can study the critical phenomena of these band-splitting transitions in the same way as the above. Further discussion will be given elsewhere.

APPENDIX: CALCULATION OF THE TIME-CORRELATION FUNCTION ξ_n

We shall show all quantities used in our calculation of the time-correlation function ξ_n. The jth interval is given by

$$I_j = \begin{cases} \left[f^{(j+1)}(0) \wedge f^{(j-1)}(0), f^{(j+1)}(0) \vee f^{(j-1)}(0) \right] & \text{for Case (I)} \quad \text{(A.1a)} \\ \left[f^{(j+2)}(0) \wedge f^{(j)}(0), f^{(j+2)}(0) \vee f^{(j)}(0) \right] & \text{for Case (II)} \quad \text{(A.1b)} \end{cases}$$

with $f^{(j)}(0) = [\alpha - (\alpha^2 - 2)(-\alpha)^{j-1}]/(\alpha + 1)$ except for $I_1 = [f(0), f^{(2)}(0)]$ of Case (I), see also Fig. 2, where the symbols $\vee$ and $\wedge$ mean to take larger one and smaller one between the two, respectively.

The jth elements of the column vectors $\mathbf{b}_k$ and $\mathbf{a}_k$ are given by

$$b_{j;k} = s_k b_{j+1;k} \quad \text{(A.2)}$$

$$= \begin{cases} \dfrac{s_k^2}{4 + (s_k^2 - 2)N^*} \dfrac{1 + s_k^{-j}}{s_k - 1} & \text{for Case (I)} \quad \text{(A.3a)} \\ \dfrac{s_k^2}{4 + (s_k^2 - 2)N^*} \dfrac{1 - s_k^{-(j+1)}}{s_k - 1} & \text{for Case (II)} \quad \text{(A.3b)} \end{cases}$$

and

$$s_{j;k} = -t_k a_{j+1;k} \quad \text{(A.4)}$$

$$= \begin{cases} \dfrac{1}{N^*}(1 - t_k^{-j}) & \text{for Case (I)} \quad \text{(A.5a)} \\ \dfrac{1}{N^*}(1 - t_k^{-(j+1)}) & \text{for Case (II)} \quad \text{(A.5b)} \end{cases}$$

where j = odd, and N^* of (3.31) has been used. Similarly, the jth elements of the row vectors $\mathbf{b}_k^*$ and $\mathbf{a}_k^*$ can be written as

$$b_{k;j}^* = \begin{cases} (s_k^2 - 2)(s_k - 1)s_k^{j-2} + \dfrac{1}{s_k}(s_k^2 - 2)\delta_{j,1} & \text{for Case (I)} \quad \text{(A.6a)} \\ (2 - s_k^2)(s_k - 1)s_k^{j-1} & \text{for Case (II)} \quad \text{(A.6b)} \end{cases}$$

and

$$a_{k;j}^* = \begin{cases} (-t_k)^j + \dfrac{t_k}{t_k + 1}\delta_{j,1} & \text{for Case (I)} \quad \text{(A.7a)} \\ -(-t_k)^{j+1} & \text{for Case (II)} \quad \text{(A.7b)} \end{cases}$$

$\mathbf{b}_k$ and $\mathbf{b}_k^*$ have been derived from the fact that $\mathbf{c}_0^* = \mathbf{b}_1^*$.

The row vectors $\mathbf{c}_1^*$ and $\mathbf{c}_2^*$ itroduced in (3.24) are given by

$$c_{1;j}^* = \begin{cases} \dfrac{\alpha}{\alpha+1} b_{1;j}^* - \dfrac{1}{2}\left(\dfrac{\alpha^2-2}{\alpha+1}\right)^2\left(1 - \dfrac{1}{\alpha^4}\right)(-\alpha^2)^j \\ \qquad - \dfrac{1}{2}\left(\dfrac{\alpha^2-2}{\alpha+1}\right)^2\left(1 - \dfrac{1}{\alpha^2}\right)\delta_{j,1} & \text{for Case (I)} \quad \text{(A.8a)} \\ \dfrac{\alpha}{\alpha+1} b_{1;j}^* + \dfrac{1}{2}\left(\dfrac{\alpha^2-2}{\alpha+1}\right)^2\left(1 - \dfrac{1}{\alpha^4}\right)(-\alpha^2)^{j+1} & \text{for Case (II)} \quad \text{(A.8b)} \end{cases}$$

and

$$c_{2;j}^* = \begin{cases} -\left(\dfrac{\alpha}{\alpha+1}\right)^2 b_{1;j}^* + \dfrac{2\alpha}{\alpha+1} c_{1;j}^* + \dfrac{1}{3}\left(\dfrac{\alpha^2-2}{\alpha+1}\right)^3\left(1 - \dfrac{1}{\alpha^6}\right)\alpha^{3j} \\ \qquad + \dfrac{1}{3}\left(\dfrac{\alpha^2-2}{\alpha+1}\right)^3\left(1 + \dfrac{1}{\alpha^3}\right)\delta_{j,1} & \text{for Case (I)} \quad \text{(A.9a)} \\ -\left(\dfrac{\alpha}{\alpha+1}\right)^2 b_{1;j}^* + \dfrac{2\alpha}{\alpha+1} c_{1;j}^* + \dfrac{1}{3}\left(\dfrac{2-\alpha^2}{\alpha+1}\right)^3\left(1 - \dfrac{1}{\alpha^6}\right)\alpha^{3(j+1)} \\ & \text{for Case (II)} \quad \text{(A.9b)} \end{cases}$$

The first and second moments of x are obtained by taking the scalar

products as

$$\langle x \rangle_f = (\mathbf{c}_1^* \cdot \mathbf{b}_1) = \frac{\alpha}{\alpha + 1} - \frac{(\alpha - 1)^2}{4 + (\alpha^2 - 2)N^*} \tag{A.10}$$

$$\langle x^2 \rangle_f = (\mathbf{c}_2^* \cdot \mathbf{b}_1) = -\left(\frac{\alpha}{\alpha + 1} \right)^2 + \frac{2\alpha}{\alpha + 1} (\mathbf{c}_1^* \cdot \mathbf{b}_1) + \frac{2(\alpha - 1)}{(\alpha + 1)\left[4 + (\alpha^2 - 2)N^*\right]} \tag{A.11}$$

Many pairs of scalar products are used in (3.26). By making use of the relations

$$(\mathbf{b}_l^* \mathscr{H}_0 \cdot \mathbf{a}_k) = -\alpha (\mathbf{b}_l^* \cdot \mathscr{H}_1 \mathbf{a}_k) + \frac{2}{\alpha} \left(\sum_{j=\text{odd}} b_{l;j}^* \right) a_{N;k}$$

$$(\mathbf{a}_k^* \cdot \mathscr{H}_0 \mathbf{b}_l) = -\alpha (\mathbf{a}_k^* \mathscr{H}_1 \cdot \mathbf{b}_l) + \frac{2}{\alpha} \left(\sum_{j=\text{odd}} a_{k;j}^* \right) b_{N;l}$$

we obtain

$$(\mathbf{b}_l^* \cdot \mathbf{a}_k) = \frac{2(s_l - 1)}{s_l + t_k} \frac{t_k^2 - 1}{N^* t_k} \tag{A.12}$$

$$(\mathbf{a}_k^* \cdot \mathbf{b}_l) = \frac{2}{t_k + s_l} \frac{s_l(s_l + 1)}{4 + (s_l^2 - 2)N^*} \tag{A.13}$$

Therefore, substituting (A.12) into (3.21), we obtain

$$\beta_{lk} = \frac{t_k^2 - 1}{N^* t_k} \frac{2(s_l - 1)}{\alpha + 1} \left(\frac{1}{\alpha s_l - t_k} - \frac{\alpha}{s_l + t_k} \right) \tag{A.14}$$

Notice that $\mathscr{H}_f$ transforms each orthogonalized polynomial of order l which is defined on I_j into a linear combination of the polynomials of the same order defined on I_k. The orthogonal relation of the polynomials of order 0 and 1 leads to

$$(\mathbf{c}_1^* \cdot \mathbf{a}_k) = -\beta_{1k} \tag{A.15}$$

By straightforward calculations we obtain

$$(\mathbf{c}_1^* \cdot \mathbf{b}_l) = \frac{\alpha}{\alpha + 1} (\mathbf{b}_1^* \cdot \mathbf{b}_l) - \frac{(\alpha - 1)^2}{s_l + \alpha^2} \frac{s_l(s_l + 1)}{4 + (s_l^2 - 2)N^*} \tag{A.16}$$

$$(\mathbf{c}_2^* \cdot \mathbf{a}_k) = -\left(\frac{\alpha}{\alpha + 1} \right)^2 (\mathbf{b}_1^* \cdot \mathbf{a}_k) + \frac{2\alpha}{\alpha + 1} (\mathbf{c}_1^* \cdot \mathbf{a}_k) + \frac{2(\alpha - 1)}{3(\alpha + 1)^2} \frac{t_k^2 - 1}{N^* t_k} \frac{\alpha^4 - 2\alpha^2 + 4}{t_k + \alpha^3} \tag{A.17}$$

Our time-correlation function (3.26) is complicated, because the amplitude of each eigenmode has summations over other eigenvalues, such as $\sum_l (\mathbf{c}_1^* \cdot \mathbf{b}_l)\beta_{lk}$ and $\sum_k \beta_{lk}(\mathbf{a}_k^* \cdot \mathbf{b}_1)$. However, the summations can easily be carried out by making use of the relation

$$\sum_{j=1}^{N} \frac{1}{x - \lambda_j} = \frac{F'(x)}{F(x)}$$

where $F(x) = \prod_{n=1}^{N}(x - \lambda_j)$. Taking the left-hand sides of (3.17) and (3.18) for $F(x)$, we obtain

$$\sum_{l=1}^{N} (\mathbf{c}_1^* \cdot \mathbf{b}_l)\beta_{lk} = \left(\frac{\alpha}{\alpha+1}\right)^2 (\mathbf{b}_1^* \cdot \mathbf{a}_k) - \frac{2\alpha}{\alpha+1}(\mathbf{c}_1^* \cdot \mathbf{a}_k) - \frac{\alpha-1}{(\alpha+1)^2} \frac{t_k^2 - 1}{N^* t_k} \frac{(\alpha^4 - 2\alpha^2 + 3)t_k^2 + 2\alpha^2(\alpha^2 - 2)}{(\alpha^3 + t_k)\left[t_k^2 + \alpha^2(\alpha^2 - 2)\right]} \tag{A.18}$$

$$\sum_{k=1}^{N} \beta_{lk}(\mathbf{a}_k^* \cdot \mathbf{b}_1) = -\frac{\alpha}{\alpha+1}(\mathbf{b}_l^* \cdot \mathbf{b}_1) + \frac{(s_l - 1)^2}{(s_l^2 + \alpha^2 - 2)} \frac{2(\alpha^2 - 1)}{4 + (\alpha^2 - 2)N^*} \tag{A.19}$$

Substituting (A.13), (A.17), and (A.18) into (3.26), we find that the amplitude of the eigenmode t_k in (3.26) takes the form

$$\frac{2\alpha(\alpha+1)(\alpha-1)^3}{4 + (\alpha^2 - 2)N^*} \frac{(1 - t_k^2)\left[t_k^2 - 2\alpha^2(\alpha^2 - 2)\right]}{3N^* t_k(\alpha + t_k)(\alpha^3 + t_k)\left[t_k^2 + \alpha^2(\alpha^2 - 2)\right]} \tag{A.20}$$

Similarly, substituting (A.16) and (A.19) into (3.26), we find that the amplitude of the eigenmode s_l can be written as

$$\frac{2(\alpha+1)(\alpha-1)^3}{4 + (\alpha^2 - 2)N^*} \frac{s_l(s_l - a)^2(s_l + 1)}{(\alpha^2 + s_l)(s_l^2 + \alpha^2 - 2)\left[4 + (s_l^2 - 2)N^*\right]} \quad \text{for} \quad l \neq 1 \tag{A.21}$$

For $l = 1$, it gives the constant term $\langle x \rangle_f^2$. After the normalization of (3.27) with the use of (A.10) and (A.11), we obtain (3.28) with (3.29) and (3.30).

REFERENCES

1. M. J. Feigenbaum, *J. Stat. Phys.* **19**:25 (1978).
2. R. M. May, *Nature* **261**:459 (1976).

3. J. Crutchfield, D. Farmer, N. Packard, R. Shaw, G. Jones, and R. J. Donnelly, *Phys. Lett.* **76A**:1 (1980); V. Franceschini and C. Tebaldi, *J. Stat. Phys.* **21**:707 (1979); V. Franceschini, *Ibid.* **22**:397 (1980); B. A. Huberman and J. P. Crutchfield, *Phys. Rev. Lett.* **43**:1743 (1979); J. M. Wersinger, J. M. Finn, and E. Ott, *Ibid.* **44**:453 (1980).
4. M. Giglio, S. Musazzi, and U. Perini, *Phys. Rev. Lett.* **47**:243 (1981); J. P. Gollub and S. V. Benson, *J. Fluid Mech.* **100**:449 (1980); J. Maurer and A. Libchaber, *J. Phys.* (*Paris*), *Lett.* **41**:L515 (1980).
5. R. Keolian, L. A. Turkevich, S. J. Putterman, I. Rudnick, and J. A. Rudnick, *Phys. Rev. Lett.* **47**:1133 (1981).
6. P. S. Linsay, *Phys. Rev. Lett.* **47**:1349 (1981).
7. W. Lauterborn and E. Cramer, *Phys. Rev. Lett.* **47**:1445 (1981).
8. H. Mori and H. Fujisaka, *Prog. Theor. Phys.* **63**:1931 (1980); M. I. Rabinovich, *Usp. Fiz. Nauk* **125**:123 (1978) [*Sov. Phys. Usp.* **21**:443 (1978)].
9. E. N. Lorenz, *J. Atmos. Sci.* **20**:130 (1963).
10. S. K. Ma, *Modern Theory of Critical Phenomena*. (W. A. Benjamin, New York, 1976).
11. M. J. Feigenbaum, *Phys. Lett.* **74A**:375 (1979).
12. B. A. Huberman and J. Rudnick, *Phys. Rev. Lett.* **45**:154 (1980); J. Crutchfield, M. Nauenberg, and J. Rudnick, *Ibid.* **46**:933 (1981); B. Shraiman, C. E. Wayne, and P. C. Martin, *Ibid.* **46**:935 (1981).
13. B. A. Huberman and A. B. Zisook, *Phys. Rev. Lett.* **46**:626 (1981); M. Nauenberg and J. Rudnick, *Phys. Rev.* **B24**:493 (1981); J. D. Farmer, *Phys. Rev. Lett.* **47**:179 (1981).
14. T. Geisel and J. Nierwetberg, *Phys. Rev. Lett.* **47**:975 (1981).
15. P. Collet, J. P. Eckmann, and O. E. Lanford, *Commun. Math. Phys.* **76**:211 (1980).
16. S. Ito, S. Tanaka, and H. Nakada, *Tokyo J. Math.* **2**:221 (1979).
17. S. Ito, S. Tanaka, and H. Nakada, *Tokyo J. Math.* **2**:241 (1979).
18. T. Yoshida, H. Mori, and H. Shigematsu, *J. Stat. Phys.* **31** (1982).
19. T. Y. Li and J. A. Yorke, *Am. Math. Monthly* **82**:985 (1975); Y. Oono, *Prog. Theor. Phys.* **59**:1028 (1978); Y. Oono and M. Oshikawa, *Ibid.* **64**:54 (1980).
20. A. Lasota and J. A. Yorke, *Trans. Am. Math. Soc.* **186**:481 (1973); T. Y. Li and J. A. Yorke, *Ibid.* **235**:183 (1978); D. Ruelle, *Commun. Math. Phys.* **55**:47 (1977).
21. J. Guckenheimer, *Commun. Math. Phys.* **70**:133 (1979).
22. N. Metropolis, M. L. Stein, and P. R. Stein, *J. Comb. Theory* (*A*) **15**:25 (1973); J. Guckenheimer, *Inventiones Math.* **39**:165 (1977).
23. Y. Oono and Y. Takahashi, *Prog. Theor. Phys.* **63**:1804 (1980).
24. D. Forster, *Hydrodynamic Fluctuations, Broken Symmetry, and Correlation Functions*. (W. A. Benjamin, New York, 1975).
25. S. Grossmann and S. Thomae, *Z. Naturforsch.* **32a**:1353 (1977).
26. H. Fujisaka and T. Yamada, *Z. Naturforsch.* **33a**:1455 (1978).
27. H. Mori, B. C. So, and T. Ose, *Prog. Theor. Phys.* **66**:1266 (1981).
28. H. Mori, T. Ose, and H. Okamoto, to be published.
29. S. J. Shenker and L. P. Kadanoff, *J. Phys. A* **14**:L23 (1981).
30. A. N. Sarkovskii, *Ukrain. Math. Z.* **16**:61 (1964); P. Stefan, *Commun. Math. Phys.* **54**:237 (1977).
31. V. I. Arnold and A. Avez, *Ergodic Problems of Classical Mechanics* (W. A. Benjamin Inc., New York, 1968).
32. J. A. Yorke and E. D. Yorke, *J. Stat. Phys.* **21**:263 (1979).